Available online at www.sciencedirect.com
SCIENCE DIRECT
Journal of Computational Physics 215 (2006) 197–218
JOURNAL OF COMPUTATIONAL PHYSICS
www.elsevier.com/locate/jcp

A local discontinuous Galerkin method for the Korteweg–de Vries equation with boundary effect

Hailiang Liu [a,*], Jue Yan [b]

[a] *Iowa State University, Mathematics Department, Carver Hall 400, Ames, IA 50011, United States*
[b] *Department of Mathematics, UCLA, Los Angeles, CA 90095, United States*

Received 30 May 2005; received in revised form 21 October 2005; accepted 25 October 2005
Available online 15 December 2005

Abstract

A local discontinuous Galerkin method for solving Korteweg–de Vries (KdV)-type equations with non-homogeneous boundary effect is developed. We provide a criterion for imposing appropriate boundary conditions for general KdV-type equations. The discussion is then focused on the KdV equation posed on the negative half-plane, which arises in the modeling of transition dynamics in the plasma sheath formation [H. Liu, M. Slemrod, KdV dynamics in the plasma-sheath transition, Appl. Math. Lett. 17(4) (2004) 401–410]. The guiding principle for selecting inter-cell fluxes and boundary fluxes is to ensure the L^2 stability and to incorporate given boundary conditions. The local discontinuous Galerkin method thus constructed is shown to be stable and efficient. Numerical examples are given to confirm the theoretical result and the capability of this method for capturing soliton wave phenomena and various boundary wave patterns.

1. Introduction

In applications the interesting phenomena frequently occur near the boundary and consequently the design of effective numerical procedures to capture the right boundary behavior is highly desirable, see e.g. [23]. In this paper we treat the Korteweg–de Vries (KdV) equation in one space dimension with an interval as the spatial domain. The KdV equation is a generic equation for the study of weakly nonlinear long waves. It arises in many physical situations, such as surface water waves, plasma waves, Rossby waves and harmonic lattices.

The KdV equation is integrable and can be solved on the infinite line using the celebrated inverse scattering approach [14]. For KdV equation posed on the infinite line, there has been several quite successful numerical methods available such as spectral/pseudospectral methods, finite difference methods as well as local discontinuous Galerkin (LDG, for short) methods developed by many authors from both theoretical and computational points of view. For initial boundary value (IBV) problems the boundary effect poses additional difficulties and requires special treatment. Among others, spectral Galerkin-type methods have been recently

* Corresponding author.
E-mail addresses: hliu@iastate.edu (H. Liu), yan@math.ucla.edu (J. Yan).

0021-9991/$ - see front matter © 2005 Elsevier Inc. All rights reserved.
doi:10.1016/j.jcp.2005.10.016

introduced by several authors to handle non-periodic boundary conditions, see e.g. [21,26,27,19,29]. However, using the spectral type method one often needs to properly choose collocation points to minimize the number of unstable modes.

In this work we are interested in developing a stable LDG method for approximating solutions of the KdV equation with non-homogeneous boundary conditions. Our discussion will focus on the following setting:

$$u_t + 6uu_x + u_{xxx} = 0, \quad x \in (-\infty, 0],$$

subject to initial data and boundary conditions

$$u(x,0) = u_0(x),$$
$$u(0,t) = a(t), \quad u_x(0,t) = b(t).$$

The negative quarter-plane (considered in $\{(x, t), x \leqslant 0, t \geqslant 0\}$) problem is of special interest to us because of several physical applications. It arises in the modeling of transition dynamics hidden in the plasma sheath formation, see [25] where the authors derived a perturbed KdV model to approximate a 1-D Euler–Poisson model for the motion of weakly ionized plasma. Another example is weakly nonlinear long waves propagating on a fluid with surface tension [22]. We note that the positive quarter-plane (considered in $\{(x, t), x \geqslant 0, t \geqslant 0\}$) problem requires only one boundary condition at $x = 0$, for which the boundary effect was studied by Chu et al. [9] numerically. A number of different physical applications exist for positive quarter-plane problem, such as the generation of waves in a shallow channel by a wave-making device or the critical withdrawal of a stratified fluid from a reservoir, see [10]. The positive quarter-plane problem was also examined via the inverse scattering method, see e.g. [8,16,15]. For the study of well-posedness of positive-quarter problems we refer to [5,2,13] and references therein. The objective of this paper is to present an efficient LDG method with incorporation of boundary conditions and to show that the method is able to capture various boundary wave phenomena, including those classified in [28].

The type of discontinuous Galerkin methods we will discuss in this paper is to use a discontinuous Galerkin finite element approximation for the spatial variables and couple with explicit, nonlinearly stable high-order Runge–Kutta method for the time discretization [30]. It was first developed for the conservation laws containing first derivatives by Cockburn et al. in a series of papers, see e.g. [11] and a review paper [12]. We should point out that, among others, one advantage of the discontinuous Galerkin method is its ability to capture the boundary behavior easily through boundary fluxes. This property is crucial for the implementation of non-homogeneous boundary conditions in this work.

For equations containing higher-order spatial derivatives, discontinuous Galerkin methods cannot be directly applied. This is because the solution space, which consists of discontinuous piecewise polynomials, is not regular enough to handle higher derivatives. This led to the invention and development of the LDG method.

The first LDG method was developed by Cockburn and Shu [11] for time-dependent convection diffusion systems. Later, this method has been successfully extended to a general KdV-type equation containing third-order derivatives [33] to PDEs with fourth and fifth spatial derivatives [34], to nonlinear Schrödinger equations [32] and other nonlinear dispersive equations [24]. However, the application of this method to boundary value problems has not been done yet and will be carried out in this paper.

The idea of local discontinuous Galerkin methods for time-dependent PDEs with higher derivatives is to rewrite the original equation as a first-order system, and only then apply the discontinuous Galerkin methods. The local auxiliary variables, introduced to approximate the derivatives of the solution, are superficial and can be easily removed for linear problems. A key ingredient for the success of such methods is the careful design of the cell interface numerical fluxes. All fluxes must be designed to guarantee stability and local solvability of the auxiliary variables.

The novel idea of the LDG method proposed in this paper is to construct proper numerical fluxes for both the interior interfaces and the boundaries. Especially the boundary fluxes are to be chosen to incorporate the imposed boundary data. One crucial difficulty when deriving the L^2 stability for the IBV problem is that we have to deal with a term like uu_{xx} on the right boundary, but u_{xx} is not known a priori. Our strategy to circumvent this difficulty is via two steps: (1) introduce an auxiliary problem with zero boundary data $u(0, t) = 0$,

with which the term uu_{xx} vanishes; (2) convert the original IBV problem with non-homogeneous boundary data to the auxiliary problem through a simple transformation. We refer to [23] for transformation methods applied to a class of linearized evolution equations.

In our LDG formulation, we construct boundary fluxes in such a way that we use the boundary data whenever it is available, and take other boundary fluxes as the value evaluated from the numerical solutions. In contrast, one often needs to assume the value u_{xx} when pursuing the inverse scattering method, see e.g. [8].

For the stability analysis we first formulate a stability criterion for the continuous model, and then justify such a stability property to be well preserved also by the numerical solution from our LDG method. We should point out that for non-homogeneous data the transformation is introduced mainly to establish the stability property of the scheme, and it is not used in real computations. The method is easily implemented and can be extended to more general equations.

The organization of the paper is as follows. In Section 2, we first discuss how to impose admissible boundary conditions for a general KdV-type equation, we then give an energy estimate for the KdV IBV problem on the negative quarter-plane. In Section 3, we describe the formulation of our LDG method and prove the nonlinear L^2 stability. Section 4 is devoted to a discussion of various wave patterns near the boundary. Numerical examples are presented in Section 5 and results are consistent with the wave patterns described. We end the paper with a few concluding remarks in Section 6.

2. Boundary conditions and well-posedness

2.1. Boundary conditions

For the KdV equation, the initial boundary value problem is often set in a quarter-plane, see for instance [1,5,3,19]. The KdV equation on a finite spatial interval has also been considered by several authors, see e.g. [4,26,29]. For the IBV problem to be well-posed one has to give proper boundary conditions. We refer to [15] for giving appropriate number of boundary conditions for linear KdV equations.

To highlight the reasoning of what boundary conditions are admissible, we start with a more general dispersive wave equation from [33]

$$u_t + f(u)_x + (r'(u)g(r(u)_x)_x)_x = 0 \tag{2.1}$$

in the strip $L \leqslant x \leqslant R$. The functions $f(u)$, $r(u)$, and $g(u)$ are arbitrary (smooth) functions. The KdV equation is a special case of (2.1) (for the choice $f(u) = 3u^2$, $g(u) = u$, and $r(u) = u$).

We prescribe an initial condition

$$u(x,0) = u_0(x),$$

and add the boundary conditions

$$u(L,t) = u(R,t) = 0.$$

The third-order derivative in space requires one more boundary condition. A formulation of a third boundary condition requires careful thoughts. This is related to the well-posedness concept of the problem. The initial boundary value problem is said to be well-posed if for all smooth compatible data there is a unique smooth solution, and in every finite time interval $0 \leqslant t \leqslant T$ the solution can be estimated in terms of the initial and boundary data, see e.g. [23].

Set

$$G(q) := \int^q g(\xi)\,\mathrm{d}\xi, \quad F(u) := \int_0^u f(\xi)\,\mathrm{d}\xi.$$

Multiplying Eq. (2.1) by u with proper regroup, we have

$$\frac{1}{2}(u^2)_t + \{uf(u) - F(u) + ur'(u)g(r(u)_x)_x - r(u)_x g(r(u)_x) + G(r(u)_x)\}_x = 0. \tag{2.2}$$

This indicates the conservation of the kinetic energy on the whole domain. However, the energy is not conserved on the finite domain because of the boundary effect. We thus need to propose proper boundary conditions so that the kinetic energy is still controllable. Note that

$$qg(q) - G(q) = \int_0^q \xi g'(\xi)\,\mathrm{d}\xi =: B(q).$$

Integration of (2.2) over $[L, R]$, using the data $u(t, L) = u(t, R) = 0$, leads to

$$\frac{1}{2}\frac{\mathrm{d}}{\mathrm{d}t}\int_L^R u^2\,\mathrm{d}x = B(r(u)_x)|_{x=R} - B(r(u)_x)|_{x=L}, \tag{2.3}$$

which is clearly bounded if u_x were given at two boundaries. However, the spatial order of the equation allows only one more boundary condition besides $u(L, t) = u(R, t) = 0$. A third boundary condition can be chosen such that the right-hand side is bounded by the given data if B is of one sign. For example, if $B(q) \geqslant 0$, the RHS of (2.3) is bounded by $B(r(u)_x)|_{x=R}$, for which $u_x(t, R)$ needs to be given; if $B(q) \leqslant 0$, $u_x(t, L)$ needs to be known.

Proposition 2.1. *Consider the IBV problem (2.1) in the domain $(L, R)\times(0, T)$, subject to $u(x, 0) = u_0(x)$ and $u(L, t) = u(R, t) = 0$. For the problem to be well-posed a third boundary condition is necessarily imposed in such a way that*

(i) *$u_x(t, R)$ is imposed for $B(q) \geqslant 0$;*
(ii) *$u_x(t, L)$ is imposed for $B(q) \leqslant 0$.*

We note that for a positive quarter-plane problem, Chu et al. [9] used an energy conservation law for KdV equation to deduce that one boundary condition should be applied at $x = 0$, with the other two being bounded conditions on the solution as $x \to \infty$. Using the above argument, one could discuss more general boundary conditions such as the form $\sum_{i=0}^{2}\alpha_i^j\partial_x^i u(x, t)$, $j = 1, 2, 3$, prescribed at $x = L, R$, see [6,7] for choices of α's for linearized KdV equations.

2.2. Half-space problem

In this paper we focus on the well-known KdV equation posed on the negative half space $\Omega = (-\infty, 0]$. Using Proposition 2.1 for boundary conditions we formulate the problem as follows:

$$\begin{cases} u_t + 6uu_x + u_{xxx} = 0, & x \in (-\infty, 0], \\ u(x, 0) = u_0(x), & x \in (-\infty, 0], \\ u(0, t) = a(t), & t > 0, \\ u_x(0, t) = b(t), & t > 0. \end{cases} \tag{2.4}$$

We seek the solution decaying at $x = -\infty$. For the equation posed on the positive half space $x > 0$, one just needs one condition $u(0, t)$ at the end $x = 0$. The existence and uniqueness of the solution for this problem may be established in the spirit of [3,4].

Our goal is to design a stable numerical method for the above IBV problem. However, we would first like, on the PDE level, to establish an energy estimate of the following form:

$$\|u(\cdot, t)\| \leqslant K(\|u_0\|, a(t), b(t)), \quad t \in [0, T],$$

where $\|\cdot\|$ is the L^2 norm and K is a proper functional. In order to obtain such a priori estimate, we first consider the following auxiliary problem with homogeneous first-order boundary condition:

$$\begin{cases} v_t + f(v,x,t)_x + v_{xxx} = 0, \\ v(x,0) = v_0(x), \\ v(0,t) = v(-\infty,t) = 0, \\ v_x(0,t) = g(t). \end{cases} \tag{2.5}$$

Assume the time–space dependent function f has the property

$$\left| \int_\Omega \partial_x \int_0^v f(s,x,t)\,\mathrm{d}s\,\mathrm{d}x \right| \leqslant K_1(t)\|v(\cdot,t)\|^2 + K_2(t), \quad t \in [0,T], \tag{2.6}$$

for $T > 0$ and some known smooth functions $K_i(t)$, $i = 1, 2$. Thus we have

Lemma 2.2. *Given $f(v, x, t)$ satisfying (2.6). Then for any $T > 0$, the smooth solution of problem (2.5) satisfies the estimate*

$$\|v(\cdot,t)\|^2 \leqslant \exp\left(2\int_0^t K_1(\tau)\mathrm{d}\tau\right)\left\{\|v_0\|^2 + \int_0^t (g^2(\tau) + 2K_2(\tau))\mathrm{d}\tau\right\}, \quad 0 \leqslant t \leqslant T. \tag{2.7}$$

Proof. Set $F(v,x,t) := \int_0^v f(s,x,t)\mathrm{d}s$. If v solves the above IBV problem, then

$$\begin{aligned} \frac{1}{2}\frac{\mathrm{d}}{\mathrm{d}t}\|v(\cdot,t)\|^2 &= (v, v_t) = (v, -f(v,x,t)_x - v_{xxx}) \\ &= -\int_\Omega \partial_x F(v,x,t)\,\mathrm{d}x - \int_\Omega \left[vf(v,x,t) - F(v,x,t) + vv_{xx} - \frac{1}{2}v_x^2\right]_x \mathrm{d}x \\ &= \frac{1}{2}v_x^2(0,t) - \int_\Omega \partial_x F(v,x,t)\,\mathrm{d}x. \end{aligned}$$

Using the boundary data and the assumption on f, we have

$$\frac{\mathrm{d}}{\mathrm{d}t}\|v(\cdot,t)\|^2 \leqslant g^2(t) + 2K_1(t)\|v(\cdot,t)\|^2 + 2K_2(t).$$

By the Gronwall inequality, the above reduces to (2.7) as desired. □

Equipped with Lemma 2.2 and through a simple transformation, we are able to derive a prior estimate for the original problem (2.4).

Set

$$u := v + \mathrm{e}^x a(t)$$

and substitute it into the equation for u, we find that v solves the auxiliary problem (2.5) with

$$g(t) := b(t) - a(t)$$

and

$$f(v,x,t) := (a(t) + a'(t))\mathrm{e}^x + 3(v + \mathrm{e}^x a(t))^2.$$

A straightforward calculation shows that (2.6) is satisfied with

$$K_1(t) := (3|a(t)| + 0.5), \quad K_2(t) = (|a(t)| + |a'(t)| + 6a^2)^2/2.$$

Note here we use the fact that $\mathrm{e}^x \leqslant 1$ on the negative half-plane.

Using the estimate in Lemma 2.2 and the substitution $v = u - \mathrm{e}^x a(t)$, we obtain the estimate for the original problem (2.4) as the following:

$$\|u(\cdot,t)\| \leqslant K(\|u_0\|, a(t), b(t) - a(t)), \quad t \in [0,T]. \tag{2.8}$$

In next section, we will show that such a stability property is preserved by the LDG numerical solution.

3. The LDG method and its L^2 stability

3.1. Review: local discontinuous Galerkin method for KdV-type equations

In [33], Yan and Shu presented and analyzed a local discontinuous Galerkin method for KdV-type equations of the form (2.1), i.e.,

$$u_t + f(u)_x + (r'(u)g(r(u)_x)_x)_x = 0, \quad x \in \Omega, \tag{3.1}$$

augmented with initial data $u(x, t = 0) = u_0(x)$, and periodic boundary conditions.

This general equation turns to be a natural extension of the KdV equation that still allows one to write a stable DG method. The idea of LDG method is to rewrite (3.1) as a first-order system,

$$\begin{cases} u_t + (f(u) + r'(u)p)_x = 0, \\ p - g(q)_x = 0, \\ q - r(u)_x = 0. \end{cases} \tag{3.2}$$

Then apply discontinuous Galerkin method on these equations. At each time step, we first compute an auxiliary variable q through last equation in (3.2), then compute variable p through the second equation with new data of q, finally coupled with the TVB Runge–Kutta method in time, we could update u through the first equation in (3.2).

We recall that the LDG method designed in [33] for initial value problem enjoys the L^2 stability of the following form:

$$\|u(\cdot, t)\|_{L^2(\Omega)} \leqslant \|u_0(\cdot)\|_{L^2(\Omega)}.$$

For the IBV problem considered in this paper we need to establish a similar stability estimate, which reflects the boundary effect.

3.2. Initial boundary value problem with LDG method

In this section we first present a detailed formulation of a local discontinuous Galerkin method for the KdV IBV problem. We then prove L^2 stability of the numerical solutions with LDG method.

The initial boundary value problem (2.4) is set in domain $(-\infty, 0]$. In real computations, we approximate the infinite domain by $\Omega = [-M, 0]$ with large enough M and impose an artificial boundary condition $u(-M, t) = u(-\infty, t) = 0$. One difficulty in deriving the L^2 stability estimate is that one has to deal with a term like uu_{xx} on the right boundary, but u_{xx} is not known a priori. As discussed in Section 2, our approach is to introduce an auxiliary problem with zero boundary data $u(0, t) = 0$, with which the term uu_{xx} vanishes. The original IBV problem with non-homogeneous boundary data is shown to be converted to this auxiliary problem by a simple transformation. With this in mind we only need to study the LDG method for the auxiliary equation with a more general function $f(u, x, t)$, subject to suitable boundary conditions.

Now consider the following equation (new solution notation $v(x, t)$):

$$v_t + f(v, x, t)_x + v_{xxx} = 0, \quad x \in \Omega, \tag{3.3}$$

subject to the initial and boundary conditions

$$\begin{cases} v(x, 0) = v_0(x), & x \in \Omega, \\ v(0, t) = 0, & t > 0, \\ v_x(0, t) = g(t), & t > 0, \\ v(-M, t) = 0, & t > 0. \end{cases} \tag{3.4}$$

We start with a brief description of the discontinuous Galerkin method. Divide the domain $\Omega = [-M, 0]$ into N computational cells, and denote the mesh by $I_j = [x_{j-1/2}, x_{j+1/2}]$ for $j = 1, \ldots, N$. The center of the cell is $x_j = (x_{j-1/2} + x_{j+1/2})/2$, and $\Delta x_j = |I_j|$. We denote by $v^+_{j+1/2}$ the value of v at $x_{j+1/2}$ evaluated from the right cell I_{j+1}, and $v^-_{j+1/2}$ the value of v at $x_{j+1/2}$ evaluated from the left cell I_j . We then define the finite dimensional space $\mathscr{V}_{\Delta x}$ as the space of piecewise polynomials of degree k in each cell, i.e.,

$$\mathscr{V}_{\Delta x} = \{v : v \in P^k(I_j) \text{ for } x \in I_j, j = 1, \ldots, N\}.$$

In a word, we seek numerical solutions in the form $v|_{I_j} = \sum_{l=0}^{k} v_j^l \phi_j^l(x)$, here $\phi_j^l(x)$ is the polynomial base function on I_j and v_j^l is the corresponding coefficient.

Now we construct an LDG method for (3.3), (3.4). With two additional auxiliary variables p and q we rewrite the equation as a first-order system

$$\begin{cases} v_t + (f(v,x,t) + p)_x = 0, \\ p - q_x = 0, \\ q - v_x = 0, \end{cases} \tag{3.5}$$

where the variable q is used to approximate v_x and p to approximate v_{xx}.

We search for a solution of (3.5) such that for any $t \in [0, T]$, $v, p, q \in \mathscr{V}_{\Delta x}$, that satisfy (3.5) in a weak sense. Hence, we multiply (3.5) by arbitrary test functions $r, w, z \in \mathscr{V}_{\Delta x}$ and integrate over I_j, after a simple integration by parts we obtain, for all $1 \leqslant j \leqslant N$,

$$\begin{aligned} &\int_{I_j} v_t r \,\mathrm{d}x - \int_{I_j} (f(v,x,t) + p) r_x \,\mathrm{d}x + (\tilde{f}(v,x,t)_{j+\frac{1}{2}} + \hat{p}_{j+\frac{1}{2}}) r^-_{j+\frac{1}{2}} - (\tilde{f}(v,x,t)_{j-\frac{1}{2}} + \hat{p}_{j-\frac{1}{2}}) r^+_{j-\frac{1}{2}} = 0, \\ &\int_{I_j} p w \,\mathrm{d}x + \int_{I_j} q w_x \,\mathrm{d}x - \hat{q}_{j+\frac{1}{2}} w^-_{j+\frac{1}{2}} + \hat{q}_{j-\frac{1}{2}} w^+_{j-\frac{1}{2}} = 0, \\ &\int_{I_j} q z \,\mathrm{d}x + \int_{I_j} v z_x \,\mathrm{d}x - \hat{v}_{j+\frac{1}{2}} z^-_{j+\frac{1}{2}} + \hat{v}_{j-\frac{1}{2}} z^+_{j-\frac{1}{2}} = 0. \end{aligned} \tag{3.6}$$

Since the solution is discontinuous on the cell interface $x_{j\pm1/2}$, we must carefully choose the so-called numerical fluxes $\tilde{f}(v,x,t)$, $\hat{p}$, $\hat{q}$, and $\hat{v}$ to enforce stability and at the same time incorporate boundary conditions. We need to follow different principles to choose the convective flux $\tilde{f}(v,x,t)$ and fluxes $\hat{p}$, $\hat{q}$, and $\hat{v}$, which are closely related to the dispersive term v_{xxx}. The test functions r, w, z are chosen to have compact support on cell I_j, and are also allowed to be discontinuous on $x_{j\pm1/2}$. Clearly at $x_{j+1/2}$, we should take r^-, w^-, z^-, which are exactly the values of r, w, z evaluated at point $x_{j+1/2}$. Similar arguments apply to $x_{j-1/2}$ also.

All numerical fluxes are defined on the cell boundary $x_{j\pm1/2}$, for the moment we simply drop the subscripts. The convective flux $\tilde{f}(v,x,t)$ is given in the form of

$$\tilde{f}(v,x,t) = \tilde{f}(v^-, v^+, x, t),$$

where $\tilde{f}(v^-, v^+, x, t)$ is a monotone flux for $f(v, x, t)$. More precisely, $\tilde{f}(v^-, v^+, x, t)$ is chosen to be (1) a Lipschitz continuous function in both arguments v^- and v^+, (2) consistent with $f(v, x, t)$ in the sense that $\tilde{f}(v, v, x, t) = f(v, x, t)$, and (3) a non-decreasing function in v^- and a non-increasing function in v^+. Also we require that $\tilde{f}(v^-, v^+, x, t)$ be uniquely defined on cell boundary $x_{j+1/2}$, which guarantees the nice conservative property. Examples of monotone fluxes which are suitable for discontinuous Galerkin methods can be found in the review paper [12] by Cockburn and Shu. Here, we simply choose the Lax–Friedrichs flux

$$\tilde{f}(v^-, v^+, x, t) := \frac{1}{2}(f(v^-, x, t) + f(v^+, x, t) - \alpha(v^+ - v^-)), \tag{3.7}$$

where $\alpha := \max_v |f_v(v, x, t)|$ for $x \in \Omega$.

We embed the boundary conditions (3.4) into the numerical flux (3.7) in such a way that at the right boundary $x_{N+1/2}$ we take $v^+ = v(0, t)$, and at the left boundary $x_{1/2}$, we take $v^- = v(-M, t)$.

It still remains to determine other numerical fluxes $\hat{p}$, $\hat{q}$, and $\hat{v}$ in (3.6). Following [33], we choose opposite signs of $\hat{p}$ and $\hat{v}$ in order to ensure the stability. The flux $\hat{q}$ has to be chosen as q^+ since the sign of the dispersive term v_{xxx} is positive, which is consistent with the admissibility criterion for boundary conditions in Proposition 2.1. Yet we also need to embed the boundary conditions into boundary fluxes for (p, q, v) whenever the boundary conditions are given.

We now define all the remaining fluxes to complete the LDG method

$$(\hat{p}_{j+\frac{1}{2}}, \hat{q}_{j+\frac{1}{2}}, \hat{v}_{j+\frac{1}{2}}) = \begin{cases} (p^+_{j+\frac{1}{2}}, q^+_{j+\frac{1}{2}}, v^-_{j+\frac{1}{2}}), & j \in 1, \ldots, N-1, \\ (p^+_{\frac{1}{2}}, q^+_{\frac{1}{2}}, v^-_{\frac{1}{2}}), & j = 0, \\ (p^-_{N+\frac{1}{2}}, q^+_{N+\frac{1}{2}}, v^+_{N+\frac{1}{2}}), & j = N, \end{cases} \tag{3.8}$$

or

$$(\hat{p}_{j+\frac{1}{2}}, \hat{q}_{j+\frac{1}{2}}, \hat{v}_{j+\frac{1}{2}}) = \begin{cases} (p^-_{j+\frac{1}{2}}, q^+_{j+\frac{1}{2}}, v^+_{j+\frac{1}{2}}), & j \in 1, \ldots, N-1, \\ (p^+_{\frac{1}{2}}, q^+_{\frac{1}{2}}, v^-_{\frac{1}{2}}), & j = 0, \\ (p^-_{N+\frac{1}{2}}, q^+_{N+\frac{1}{2}}, v^+_{N+\frac{1}{2}}), & j = N. \end{cases} \tag{3.9}$$

For the three given boundary conditions in (3.4), the corresponding boundary fluxes are defined as follows:

$$\hat{v}_{1/2} = v^-_{1/2} = 0, \quad \hat{v}_{N+1/2} = v^+_{N+1/2} = 0, \quad \hat{q}_{N+1/2} = q^+_{N+1/2} = g(t). \tag{3.10}$$

For other cases we simply take boundary fluxes as the value evaluated from the inside of the cell as listed in (3.8). We note that in what follows, we proceed by simply using (3.8), though we can also use (3.8) for both the stability analysis and the numerical experiment.

3.3. Stability analysis

We claim that the LDG method defined above is L^2 stable.

Proposition 3.1. *The L^2 norm of the solution of (3.6)–(3.10) is bounded by initial and boundary conditions as*

$$\|v(\cdot,t)\| \leqslant \mathrm{e}^{2\int_0^t K_1(s)(s)\,\mathrm{d}s}\left[\|v_0(\cdot)\| + \int_0^t [g^2(s) + 2K_2(s)]\,\mathrm{d}s\right] \quad \forall t \in [0,T],$$

provided $f(v, x, t)$ satisfies

$$\left|\int_\Omega \partial_x \int_0^v f(s,x,t)\,\mathrm{d}s\,\mathrm{d}x\right| \leqslant K_1(t)\|v(\cdot,t)\| + K_2(t). \tag{3.11}$$

Proof. Since (3.6) holds for any test function in $\mathscr{V}_{\Delta x}$, in particular we can choose $r = v$, $w = q$, and $z = -p$. Let $F(v, x, t) = \int^v f(s, x, t)\,\mathrm{d}s$. We have

$$f(v,x,t)v_x(x,t) = \frac{\partial F}{\partial v}(v,x,t)v_x(x,t) = \frac{\mathrm{d}F}{\mathrm{d}x}(v,x,t) - \frac{\partial F}{\partial x}(v,x,t).$$

With these test functions, Eq. (3.6) becomes

$$\begin{aligned} &\int_{I_j} v_t v\,\mathrm{d}x - \int_{I_j} \frac{\mathrm{d}F}{\mathrm{d}x}(v,x,t)\,\mathrm{d}x + \int_{I_j} \frac{\partial F}{\partial x}(v,x,t)\,\mathrm{d}x - \int_{I_j} p v_x\,\mathrm{d}x \\ &\quad + \tilde{f}(v,x,t)_{j+\frac{1}{2}} v^-_{j+\frac{1}{2}} - \tilde{f}(v,x,t)_{j-\frac{1}{2}} v^+_{j-\frac{1}{2}} + \hat{p}_{j+\frac{1}{2}} v^-_{j+\frac{1}{2}} - \hat{p}_{j-\frac{1}{2}} v^+_{j-\frac{1}{2}} = 0, \\ &\int_{I_j} pq\,\mathrm{d}x + \frac{1}{2}\int_{I_j} (q^2)_x\,\mathrm{d}x - \hat{q}_{j+\frac{1}{2}} q^-_{j+\frac{1}{2}} + \hat{q}_{j-\frac{1}{2}} q^+_{j-\frac{1}{2}} = 0, \\ &-\int_{I_j} qp\,\mathrm{d}x - \int_{I_j} v p_x\,\mathrm{d}x + \hat{v}_{j+\frac{1}{2}} p^-_{j+\frac{1}{2}} - \hat{v}_{j-\frac{1}{2}} p^+_{j-\frac{1}{2}} = 0. \end{aligned} \tag{3.12}$$

Adding three equations in (3.12) and summing over all j, we obtain

$$\begin{aligned}
&\int_\Omega v_t v\,\mathrm{d}x + \sum_j \left(-F(v^-_{j+\frac{1}{2}},x,t) + F(v^+_{j-\frac{1}{2}},x,t) + \tilde f_{j+\frac{1}{2}} v^-_{j+\frac{1}{2}} - \tilde f_{j-\frac{1}{2}} v^+_{j-\frac{1}{2}}\right)\\
&\quad + \sum_j \left(\frac{1}{2}(q^-_{j+\frac{1}{2}})^2 - \frac{1}{2}(q^+_{j-\frac{1}{2}})^2 - \hat q_{j+\frac{1}{2}} q^-_{j+\frac{1}{2}} + \hat q_{j-\frac{1}{2}} q^+_{j-\frac{1}{2}}\right)\\
&\quad + \sum_j \left(-(vp)^-_{j+\frac{1}{2}} + (vp)^+_{j-\frac{1}{2}} + \hat p_{j+\frac{1}{2}} v^-_{j+\frac{1}{2}} - \hat p_{j-\frac{1}{2}} v^+_{j-\frac{1}{2}} + \hat v_{j+\frac{1}{2}} p^-_{j+\frac{1}{2}} - \hat v_{j-\frac{1}{2}} p^+_{j-\frac{1}{2}}\right)\\
&\quad = -\int_\Omega \frac{\partial F}{\partial x}(v,x,t)\,\mathrm{d}x. \qquad (3.13)
\end{aligned}$$

Now we regroup (3.13) with interior and boundary terms denoted by I^I and I^B,

$$\frac{1}{2}\frac{\mathrm{d}}{\mathrm{d}t}\|v(\cdot,t)\|^2_{L^2(\Omega)} + I^I + I^B = -\int_\Omega \frac{\partial F}{\partial x}(v,x,t)\,\mathrm{d}x, \qquad (3.14)$$

where I^I is defined by (for simplicity we drop subscripts $j+\frac{1}{2}\in\Omega^I$, the interior of domain Ω)

$$\begin{aligned}
I^I &= \sum_{\Omega^I}\left(-F(v^-,x,t) + F(v^+,x,t) + \tilde f(v,x,t)v^- - \tilde f(v,x,t)v^+\right) + \sum_{\Omega^I}\left(\frac{1}{2}(q^-)^2 - \frac{1}{2}(q^+)^2 - \hat q q^- + \hat q q^+\right)\\
&\quad + \sum_{\Omega^I}\left(-(vp)^- + (vp)^+ + \hat p v^- - \hat p v^+ + \hat v p^- - \hat v p^+\right),
\end{aligned}$$

and I^B collects all boundary terms,

$$\begin{aligned}
I^B &= \left(-F(v^-_{N+\frac{1}{2}},x_{N+\frac{1}{2}},t) + F(v^+_{\frac{1}{2}},x_{\frac{1}{2}},t) + \tilde f(v,x,t)_{N+\frac{1}{2}} v^-_{N+\frac{1}{2}} - \tilde f(v,x,t)_{\frac{1}{2}} v^+_{\frac{1}{2}}\right)\\
&\quad + \left(\frac{1}{2}(q^-_{N+\frac{1}{2}})^2 - \frac{1}{2}(q^+_{\frac{1}{2}})^2 - \hat q_{N+\frac{1}{2}} q^-_{N+\frac{1}{2}} + \hat q_{\frac{1}{2}} q^+_{\frac{1}{2}}\right)\\
&\quad + \left(-(vp)^-_{N+\frac{1}{2}} + (vp)^+_{\frac{1}{2}} + \hat p_{N+\frac{1}{2}} v^-_{N+\frac{1}{2}} - \hat p_{\frac{1}{2}} v^+_{\frac{1}{2}} + \hat v_{N+\frac{1}{2}} p^-_{N+\frac{1}{2}} - \hat v_{\frac{1}{2}} p^+_{\frac{1}{2}}\right).
\end{aligned}$$

We note that, besides domain boundaries $x_{\frac{1}{2}} = -M$ and $x_{N+\frac{1}{2}} = 0$, all interior cell interfaces $x_{j+\frac{1}{2}}$ for $j = 1,\ldots,N-1$ have two values contributed from left and right cells. This explains why only one-side terms present in I^B.

We now show that $I^I \geqslant 0$. Using the numerical fluxes $\hat p, \hat q, \hat v, \tilde f(v)$, as described in (3.7) or (3.8), we find that all terms related to vp are canceled. This with the relation $F(v,x,t) = \int^v f(s,x,t)\,\mathrm{d}s$ gives

$$I^I = \sum_{\Omega^I}\left(\int_{v^-}^{v^+}(f(s,x,t) - \tilde f(v,x,t))\,\mathrm{d}s + \frac{1}{2}(q^- - q^+)^2\right) \geqslant 0,$$

where we have used the consistency and monotonicity of the flux $\tilde f(v,x,t)$ to ensure the following

$$\int_{v^-}^{v^+}(f(s,x,t) - \tilde f(v,x,t))\,\mathrm{d}s = \int_{v^-}^{v^+}(\tilde f(s,s,x,t) - \tilde f(v^-,v^+,x,t))\,\mathrm{d}s \geqslant 0.$$

We now turn to estimate I^B. Using boundary fluxes defined in (3.8) and (3.10), we simplify all terms involving the right boundary $x_{N+1/2}$ as follows:

$$
\begin{aligned}
&-F(v^-_{N+\frac{1}{2}},x,t)+\tilde{f}(v,x,t)_{N+\frac{1}{2}}v^-_{N+\frac{1}{2}}\\
&\quad=F(v^+_{N+\frac{1}{2}},x,t)-F(v^-_{N+\frac{1}{2}},x,t)+\tilde{f}(v,x,t)_{N+\frac{1}{2}}v^-_{N+\frac{1}{2}}-\tilde{f}(v,x,t)_{N+\frac{1}{2}}v^+_{N+\frac{1}{2}}\\
&\quad=\int_{v^-_{N+\frac{1}{2}}}^{v^+_{N+\frac{1}{2}}}(f(s,x,t)-\tilde{f}(v,x,t)_{N+\frac{1}{2}})\,\mathrm{d}s>0,\\
&\frac{1}{2}(q^-_{N+\frac{1}{2}})^2-\hat{q}_{N+\frac{1}{2}}q^-_{N+\frac{1}{2}}=\frac{1}{2}(q^-_{N+\frac{1}{2}}-q^+_{N+\frac{1}{2}})^2-\frac{1}{2}(q^+_{N+\frac{1}{2}})^2>-\frac{1}{2}g(t)^2\\
&-(vp)^-_{N+\frac{1}{2}}+\hat{p}_{N+\frac{1}{2}}v^-_{N+\frac{1}{2}}+\hat{v}_{N+\frac{1}{2}}p^-_{N+\frac{1}{2}}=0.
\end{aligned}
$$

Similarly terms involving the left boundary $x_{1/2}$ reduce to

$$
\begin{aligned}
&F(v^+_{\frac{1}{2}},x,t)-\tilde{f}(v,x,t)_{\frac{1}{2}}v^+_{\frac{1}{2}}=\int_{v^-_{\frac{1}{2}}}^{v^+_{\frac{1}{2}}}(f(s,x,t)-\tilde{f}(v,x,t)_{\frac{1}{2}})\,\mathrm{d}s>0,\\
&-\frac{1}{2}(q^+_{\frac{1}{2}})^2+\hat{q}_{\frac{1}{2}}q^+_{\frac{1}{2}}=\frac{1}{2}\left(q^+_{\frac{1}{2}}\right)^2>0,\\
&(vp)^+_{\frac{1}{2}}-\hat{p}_{\frac{1}{2}}v^+_{\frac{1}{2}}-\hat{v}_{\frac{1}{2}}p^+_{\frac{1}{2}}=0.
\end{aligned}
$$

Collecting all terms estimated above, we have

$$
I^B\geqslant-\frac{1}{2}g(t)^2.
$$

This with $I^I\geqslant 0$ and the assumption (3.11) leads equality (3.14) to

$$
\frac{1}{2}\frac{\mathrm{d}}{\mathrm{d}t}\|v(\cdot,t)\|\leqslant K_1(t)\|v(\cdot,t)\|+\frac{1}{2}g(t)^2+K_2(t).
$$

By the Gronwall inequality, we obtain the desired estimate. □

Equipped with the above L^2 estimate, we turn to establish the stability for the LDG method applied to the original problem. Let $u(x,t)$ denote the solution of original problem (2.4). As discussed in Section 2, we use the transformation $v(x,t)=u(x,t)-\mathrm{e}^x a(t)$ such that $v(x,t)$ satisfies the auxiliary problem (2.5), i.e. (3.4) on the computational domain $[-M,0]$. Applying the L^2 estimate stated in Proposition 3.1 we are able to summarize the L^2 stability of LDG method for the IBV problem (2.4) as follows.

Theorem 3.1. *The L^2 norm of the numerical solution of (2.4) is bounded by the initial and boundary data*

$$
\|u(\cdot,t)\|_{L^2(\Omega)}\leqslant K(a(t),b(t),\|u_0\|_{L^2(\Omega)})\quad\forall t\in[0,T].
$$

We would like to specify the fact that the transformation is introduced mainly for the purpose of L^2 stability analysis, we do not use it in real computations. To avoid any confusion, we simply reclaim the LDG scheme for problem (2.4). Let $f(u)=3u^2$. With two auxiliary variables q and p, we rewrite the KdV equation into a first-order system,

$$
\begin{cases}
u_t+(f(u)+p)_x=0,\\
p-q_x=0,\\
q-u_x=0.
\end{cases}
\tag{3.15}
$$

Then apply the discontinuous Galerkin method on the system. For convection term, we choose the Lax–Friedrichs flux,

$$
\tilde{f}(u^-,u^+):=\frac{1}{2}(f(u^-)+f(u^+)-\alpha(u^+-u^-)),
\tag{3.16}
$$

where $\alpha:=\max_u|f_u(u)|$ for $x\in\Omega$, and the numerical fluxes for q,p,u are

$$(\hat{p}_{j+\frac{1}{2}}, \hat{q}_{j+\frac{1}{2}}, \hat{u}_{j+\frac{1}{2}}) = \begin{cases} (p^+_{j+\frac{1}{2}}, q^+_{j+\frac{1}{2}}, u^-_{j+\frac{1}{2}}), & j \in 1, \ldots, N-1, \\ (p^+_{\frac{1}{2}}, q^+_{\frac{1}{2}}, u^-_{\frac{1}{2}}), & j = 0, \\ (p^-_{N+\frac{1}{2}}, q^+_{N+\frac{1}{2}}, u^+_{N+\frac{1}{2}}), & j = N. \end{cases} \tag{3.17}$$

To impose the given boundary conditions in (2.4), the corresponding boundary fluxes are defined as

$$\hat{u}_{1/2} = u^-_{1/2} = 0, \quad \hat{u}_{N+1/2} = u^+_{N+1/2} = a(t), \quad \hat{q}_{N+1/2} = q^+_{N+1/2} = b(t). \tag{3.18}$$

All numerical examples in Section 5 are based on the above fluxes choices. Similar results can be obtained if we choose the other alternative fluxes $p^-_{j+\frac{1}{2}}$ with $u^+_{j+\frac{1}{2}}$ for $j \in 1, \ldots, N-1$, as given in (3.9).

3.4. Possible extensions

The methodology taken here can be extended in various ways. For instance, for the KdV equation posed on a finite domain $x \in [L, R]$, with boundary conditions

$$\begin{cases} u_t + 6uu_x + u_{xxx} = 0, & x \in [L, R], \\ u(x, 0) = u_0(x), & x \in [L, R], \\ u(L, t) = a_1(t), \ \ u(R, t) = a_2(t), & t > 0, \\ u_x(R, t) = b(t), & t > 0. \end{cases}$$

We apply a transformation of the form

$$u = v + \frac{a_2 - a_1}{R - L}x + \frac{Ra_1 - La_2}{R - L},$$

to convert the above problem to an auxiliary problem with the following data:

$$v(L, t) = v(R, t) = 0, \quad v_x(R, t) = b(t) - \frac{a_2(t) - a_1(t)}{R - L},$$

to which our proposed method can be applied.

This transformation also applies to a more general equation

$$u_t + f(u)_x + (r\prime(u)g(r(u)_x)_x)_x = 0,$$

posed on a finite domain $x \in [L, R]$. According to Proposition 2.1, for the case $B(u) \leqslant 0$, the admissible side conditions are

$$u(L, t) = a_1(t), \quad u(R, t) = a_2(t), \quad u_x(L, t) = b(t), \qquad t > 0.$$

In this case, the above transformation still leads to an auxiliary problem with homogeneous data $v(L, t) = v(R, t) = 0$.

4. Wave patterns near boundary

The solution behavior of the KdV equation on the infinite line may well exist in the boundary pattern formation. The boundary effect will force some waves generated from the boundary to proceed by a transient front to match waves induced from the initial data. A particular solution of the KdV equation is the conoidal wave solution [31] expressed in terms of the mean height $\bar{u}$, the amplitude A, phase shift ϕ, wave number and dispersion relation. A special case of the conoidal wave solution is the soliton solution

$$u = \bar{u} + 2A\,\mathrm{sech}^2\sqrt{A}[x - (6\bar{u} + 4A)t + \phi]. \tag{4.1}$$

For constant boundary data five different approximate wave patterns are recently studied by Marchant and Smyth [28]. Transient solutions are constructed based on modulation theory for the KdV equation, which was derived by Whitham [31]. The modulation equations give a simple wave solution, called an undular bore, first derived by Gurevich and Pitaevskii [20] and Fornberg and Whitham [17]. Such a wave solution is formed

as an expansion fan on the characteristics, which links a level A_1 ahead of the bore to a level A_2 behind the bore for $A_2 > A_1$. The range of the bore is

$$(12A_1 - 6A_2)t \leqslant x \leqslant 4A_2 + 2A_1, \quad 0 \leqslant m \leqslant 1,$$

on which

$$u = \bar{u} + 2A[m^{-1} - 1 - m^{-1}P(m) + \mathrm{cn}^2\left(\frac{K(m)(kx - \omega + \phi)}{\pi}\right)$$

with

$$\bar{u} = (A_2 - A_1)m + 2A_1 - A_2 + 2(A_2 - A_1)P(m), \quad A = (A_2 - A_1)m,$$
$$k = \frac{\pi}{K(m)}\sqrt{A_2 - A_1}, \quad \omega = 6\bar{u}k + 4Ak(2m^{-1} - 1 - 3m^{-1}P(m)).$$

Here 'cn' is the Jacobian elliptic cosine function of parameter m. $P(m) = E(m)/K(m)$ with $K(m)$ and $E(m)$ being complete elliptic integrals of the first and second kinds, respectively. At the leading edge $m = 1$ solitons of amplitude $2(A_2 - A_1)$ occur.

For the case $A_2 < A_1$, one sees a resolution of a step down in mean height, such a solution is the mean height variation and given by

$$u = \frac{x}{6t}, \quad 6A_2 t \leqslant x \leqslant 6A_1 t,$$

with $u = A_1$ for $x > 6A_1 t$ and $u = A_2$ for $x < 6A_2 t$. This is in contrast to the undular bore solution which is the resolution of a step up in mean height. Both transition waves are constructed in [17] for step initial conditions.

Here below we recall briefly results obtained in [28] about five asymptotic wave patterns subject to constant initial and boundary data, say $a(t) = a \in \mathbb{R}$, $b(t) = 0$ and $u_0(x) = u_0 \in \mathbb{R}$.

For positive a, the soliton (4.1) can be made steady by taking $\bar{u} = -2A/3$. The steady soliton profile satisfying boundary conditions is

$$u^* = -\frac{1}{2}a + \frac{3}{2}a\,\mathrm{sech}^2\frac{1}{2}\sqrt{3a}x \to -a/2, \quad u^*(0) = a, \quad u_x^*(0) = 0.$$

But $u^* \to -a/2$ as $x \to -\infty$ does not satisfy the initial condition. Following [28] one can match this steady wave onto transient front. More precisely the approximate wave profile has the following cases:

- If $u_0 \leqslant -a/2$, a step down is made by the mean height variation, the approximate solution is

$$u = \begin{cases} u^*, & -3at \leqslant x \leqslant 0, \\ \frac{x}{6t}, & 6u_0 t \leqslant x < -3at, \\ u_0, & x < 6u_0 t. \end{cases} \tag{4.2}$$

- If $a/4 \geqslant u_0 > -a/2$, one sees a step up in mean height via an undular bore

$$u = \begin{cases} u^*, & (4u_0 - a)t \leqslant x \leqslant 0, \\ \text{undular bore}, & -6(u_0 + a)t \leqslant x \leqslant (4u_0 - a)t, \\ u_0, & x < -6(a + u_0)t. \end{cases} \tag{4.3}$$

- if $a \geqslant u_0 > a/4$, the undular bore would propagate into $x > 0$, which is clearly not possible. In this case a steady conoidal wave is formed near the boundary, matched by a partial undular bore ($0 \leqslant m \leqslant m_0 < 1$) in order to bring the mean level up to u_0 and so satisfy the initial condition

$$u = \begin{cases} \text{steady conoidal wave}, & r_f t \leqslant x \leqslant 0, \\ \text{partial undular bore}, & 6(u_0 - 2A_0/m_0)t \leqslant x \leqslant r_f t \\ u_0, & x \leqslant 6(u_0 - 2A_0/m_0)t, \end{cases} \tag{4.4}$$

where $m_0 = \frac{2(a-u_0)}{a+2u_0}$, $A_0 = a - u_0$ and

$$r_f = 6u_0 + 2A_0 - 4A_0 m_0^{-1} - \frac{4A_0(1-m_0)}{P(m_0)-(1-m_0)}.$$

- If $u_0 > a$, the wave pattern is similar to the case $a \geqslant u_0 > a/4$. In this case, the conoidal wave train has modulus $0 \leqslant m_0 \leqslant 0.5$.For the negative a, one still takes $\bar{u} = -2A/3$ to make a steady wave. Boundary conditions require $\phi = \infty$, so near boundary one only sees the uniform shelf $u^* = a$. The further matching to the initial condition is determined in the similar manner.
- If $u_0 \leqslant a < 0$, the solution is in the following form:

$$u = \begin{cases} a, & 6at \leqslant x \leqslant 0, \\ \frac{x}{6t}, & 6u_0 t \leqslant x < 6at, \\ u_0, & x < 6u_0 t. \end{cases} \tag{4.5}$$

- If $a \leqslant u_0 \leqslant -a/2$, then the solution is

$$u = \begin{cases} a, & 2(a+2u_0)t \leqslant x \leqslant 0, \\ \text{undular bore}, & 6(2a-u_0)t < x < 2(a+2u_0)t, \\ u_0, & x < 6(2a-u_0)t. \end{cases} \tag{4.6}$$

- If $u_0 > -\frac{1}{2}a$, the solution in this regime is a steady conoidal wave matched to a partial undular bore as given in (4.4). In this case the conoidal wave train has modulus $0.5 \leqslant m_0 \leqslant 1$.

The above cases tell us that there are five qualitatively different types of approximate solutions of the negative quarter-plane problem (2.4). The particular solution depends on the relation between initial and boundary values.

We point out that the dispersive nature of the equation suggests that the real solution may oscillate around the constructed approximate solution, in particular at transition points of different waves. These wave patterns are well resolved by our LDG method to be presented in next section.

5. Numerical examples

In this section we present a few numerical examples to demonstrate the accuracy and capacity of the LDG method described in Section 3. For temporal discretization, we use an explicit, nonlinearly stable third-order Runge–Kutta method [30]. Other ODE solvers can be used instead. We would like to first illustrate the high-order accuracy of the method through examples I and II, propagation and interaction of solitons. Then we would like to show the ability of the method in capturing various boundary wave patterns, through cases with constant initial and boundary data, where approximate solutions are outlined in Section 4. Note the computational domain is set to be $[-M, 0]$. We choose a suitable M to fit in with different examples.

5.1. One soliton propagation and a two soliton collision

We use single solitary wave propagation and double solitary waves interaction to test the high-order accuracy of the LDG method.

Example I. We compute the classical soliton solution of the KdV equation in $[-10, 0]$. The initial condition is given by

$$u(x,0) = 2\,\mathrm{sech}^2(x+4),$$

and the exact solution is

$$u(x,t) = 2\,\mathrm{sech}^2(x+4-ct), \quad c = 4.$$

For boundary conditions $u(-M, t)$, $u(0, t)$ and $u_x(0, t)$, we simply use the values extracted from the exact solution. The L^2 and L^∞ errors are obtained in Table 1 for $t = 0.75$. We can clearly see the method with P^k element

Table 1
Computational domain Ω is $[-10, 0]$

k		$N = 20$	$N = 40$		$N = 80$		$N = 160$	
		Error	Error	Order	Error	Order	Error	Order
1	L^2	4.34e−02	6.35e−03	2.7	1.14e−03	2.4	3.00e−04	1.9
	L^∞	1.48e−01	2.73e−02	2.4	9.82e−03	1.5	2.85e−03	1.8
2	L^2	1.66e−03	2.14e−04	2.9	2.65e−05	3.0	3.24e−06	3.0
	L^∞	1.49e−02	2.12e−03	2.8	2.66e−04	3.0	3.33e−05	3.0

$u(x, 0) = 2\,\mathrm{sech}^2(x - 4.0)$. L^2 and L^∞ errors. LDG method with $k = 1, 2$ at $t = 0.75$.

gives a uniform $(k + 1)$th order of accuracy. Note the single soliton propagates to the right with speed $c = 4$. At $t = 0.75$, one-third of the solitary wave is absorbed into the right boundary. The solution value at the right boundary is thus of O(1) and non-ignorable. We also draw the space–time 2-D graph in Fig. 1.

Example II. In this example we study the interaction of two solitary waves. The initial data is given by

$$u_0(x) = 5\frac{4.5\,\mathrm{csch}^2 1.5(x + 14.5) + 2\,\mathrm{sech}^2(x + 12)}{\{3\coth 1.5(x + 14.5) - 2\tanh(x + 12)\}^2}. \tag{5.1}$$

The exact solution is

$$u(x, t) = 5\frac{4.5\,\mathrm{csch}^2 1.5(x - 9t + 14.5) + 2\,\mathrm{sech}^2(x - 4t + 12)}{\{3\coth 1.5(x - 9t + 14.5) - 2\tanh(x - 4t + 12)\}^2}.$$

We refer to [18] for the derivation of a class of solutions of this type. Similar to previous example, we extract the three required boundary conditions from the exact solution. The interaction process can be visualized from a series of snapshots: $t = 0$ (two peaks), $t = 0.1$ (approach), $t = 0.5$ (overlap), $t = 0.6$ (depart) and $t = 1$ (post-interaction). The space–time 2-D graph is given in Fig. 2. In Tables 2 and 3, we compute the L^2 and L^∞ errors at time $t = 0.5$ during the interaction and at time $t = 1.5$ after the interaction. Note that though this particular KdV solution is smooth, it has the limit of $\frac{\infty}{\infty}$ as x approaches $9t - 14.5$ (around the peak of the bigger wave). In connection to such a peculiar behavior, we observe a very narrow wave with huge amplitude in the picture of $\frac{\partial^4 u(x,t)}{\partial x^4}$ at $t = 0$ in Fig. 3. From the linear dispersive equation error analysis, Proposition 2.4 in [33], we see to obtain a $(k + 1/2)$th order of accuracy the exact solution needs to have a smoothness up to the $(k + 3)$th derivatives. This might in some sense explain the sub-optimal order of accuracy obtained in Tables 2 and 3.

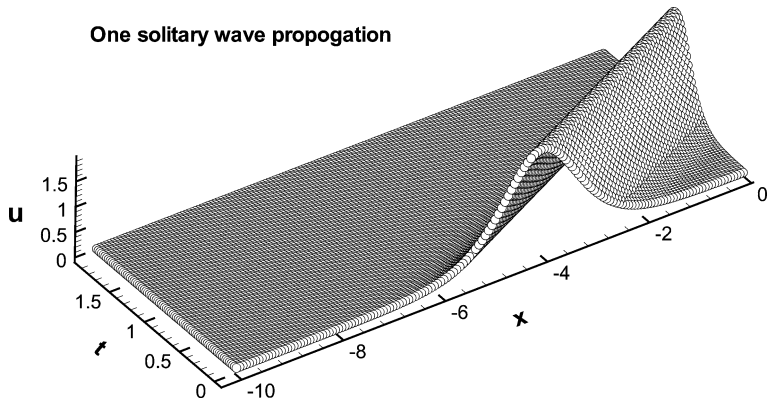

Fig. 1. Space–time graph of the solution up to $t = 2$, with P^1 polynomial and 160 cells.

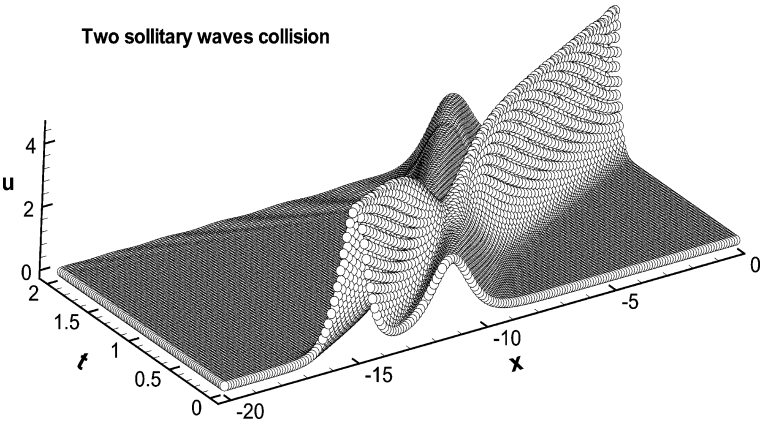

Fig. 2. Initial data is given in (5.1). P^1 polynomial and 400 cells, space–time graph of the solution up to $t = 2$.

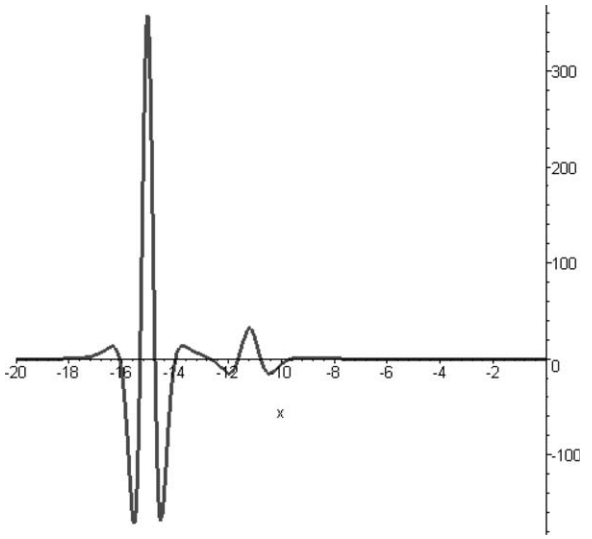

Fig. 3. Fourth spatial derivative of the exact solution $\frac{\partial^4 u(x,t)}{\partial x^4}$ at $t = 0$.

5.2. Boundary wave patterns

In the following series of examples, we would like to numerically capture the five wave patterns discussed in Section 4. Thus we choose suitable constant initial and boundary data as required in Section 4. Here we need to take big enough M to simulate ∞, and with an artificial left boundary condition $u(-M, t) = 0$.

Table 2
Computational domain Ω is $[-17, -5]$

k		$N = 120$	$N = 240$		$N = 360$		$N = 480$	
		Error	Error	Order	Error	Order	Error	Order
1	L^2	1.62e−03	3.19e−04	2.3	1.789e−04	1.4	1.14e−03	1.6
	L^∞	6.87e−03	2.78e−03	1.3	1.42e−03	1.7	8.46e−04	1.8
2	L^2	2.41e−03	6.04e−04	2.0	2.68e−04	2.0	1.51e−04	2.0
	L^∞	7.34e−03	1.81e−03	2.0	8.00e−04	2.0	4.50e−04	2.0

Initial condition is given in (5.1). L^2 and L^∞ errors in smooth domain $[-17, -11] \cup [-9, -5]$. LDG methods with $k = 1, 2$ at $t = 0.5$. During the two soliton collision.

Table 3
Computational domain Ω is $[-17, -5]$

k		$N = 120$	$N = 240$		$N = 360$		$N = 480$	
		Error	Error	Order	Error	Order	Error	Order
1	L^2	7.28e−03	3.11e−04	4.5	1.66e−04	1.5	1.02e−04	1.6
	L^∞	1.50e−02	1.42e−03	3.4	7.33e−04	1.6	4.82e−04	1.5
2	L^2	5.54e−03	1.39e−03	2.0	6.20e−04	2.0	3.48e−04	2.0
	L^∞	1.03e−02	2.59e−03	2.0	1.15e−03	2.0	6.47e−04	2.0

Initial condition is given in (5.1). L^2 and L^∞ errors. LDG methods with $k = 1, 2$ at $t = 1.5$. After the collision.

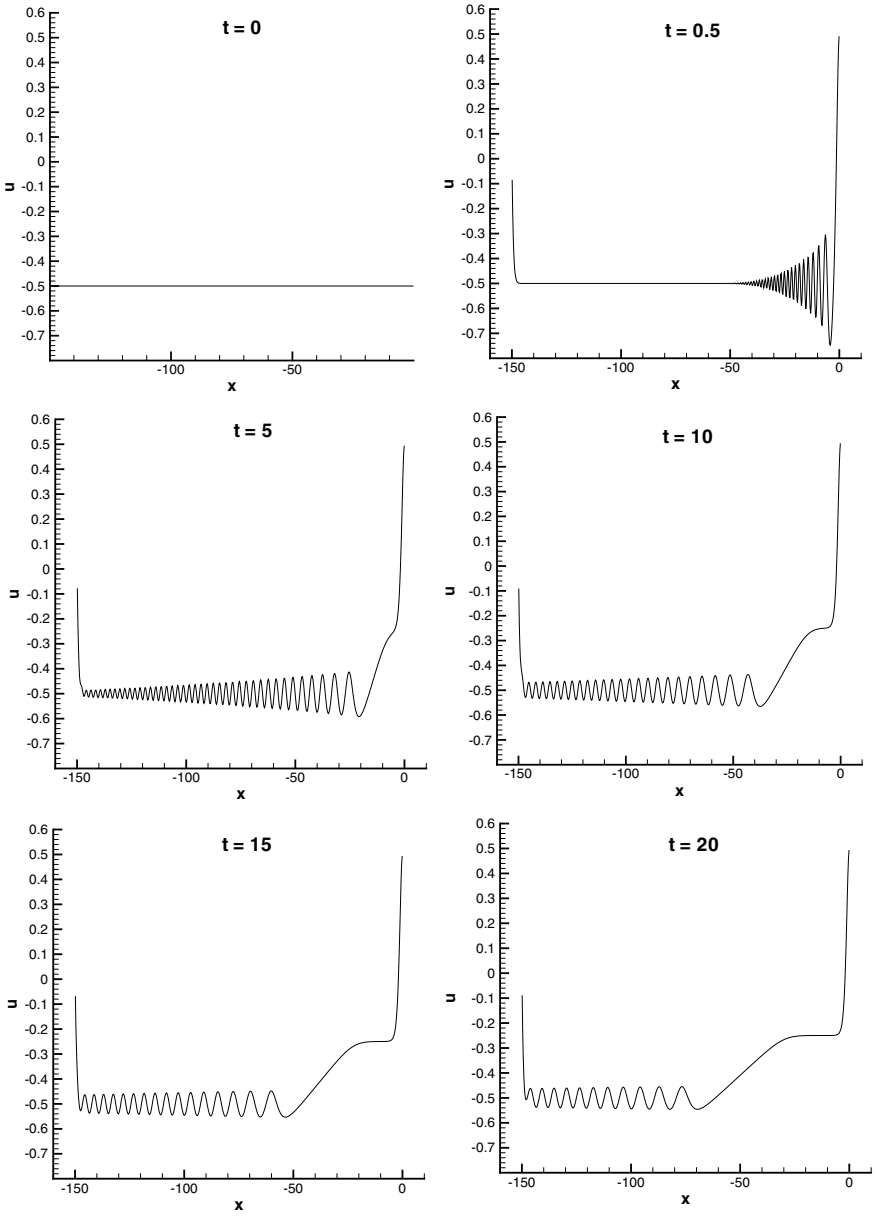

Fig. 4. $u_0(x) = -0.5$, $u(-150, t) = 0$, $u(0, t) = 0.5$, $u_x(0, t) = 0$ with P^1 polynomial and 600 cells, at $t = 0$, 0.5, 5, 10, 15, and 20.

Example III. The initial and boundary data are in the form of

$$\begin{cases} u_0(x) = -0.5, & x \in [-150, 0], \\ a(t) = 0.5, & t > 0, \\ b(t) = 0, & t > 0. \end{cases} \tag{4.2}$$

As we see the right boundary condition $a(t) = 0.5$ is positive and its relation to initial data satisfies $u_0 < -\frac{a}{2}$, so the wave pattern should have the form (4.2). Our numerical solution is shown in Fig. 4. As we observe, a single wave emerged from the right boundary, a mean height variation is formed in the middle to connect to the left smaller initial data, and for $x < 6u_0t$, the solution behaves more or less like a constant close to the initial value.

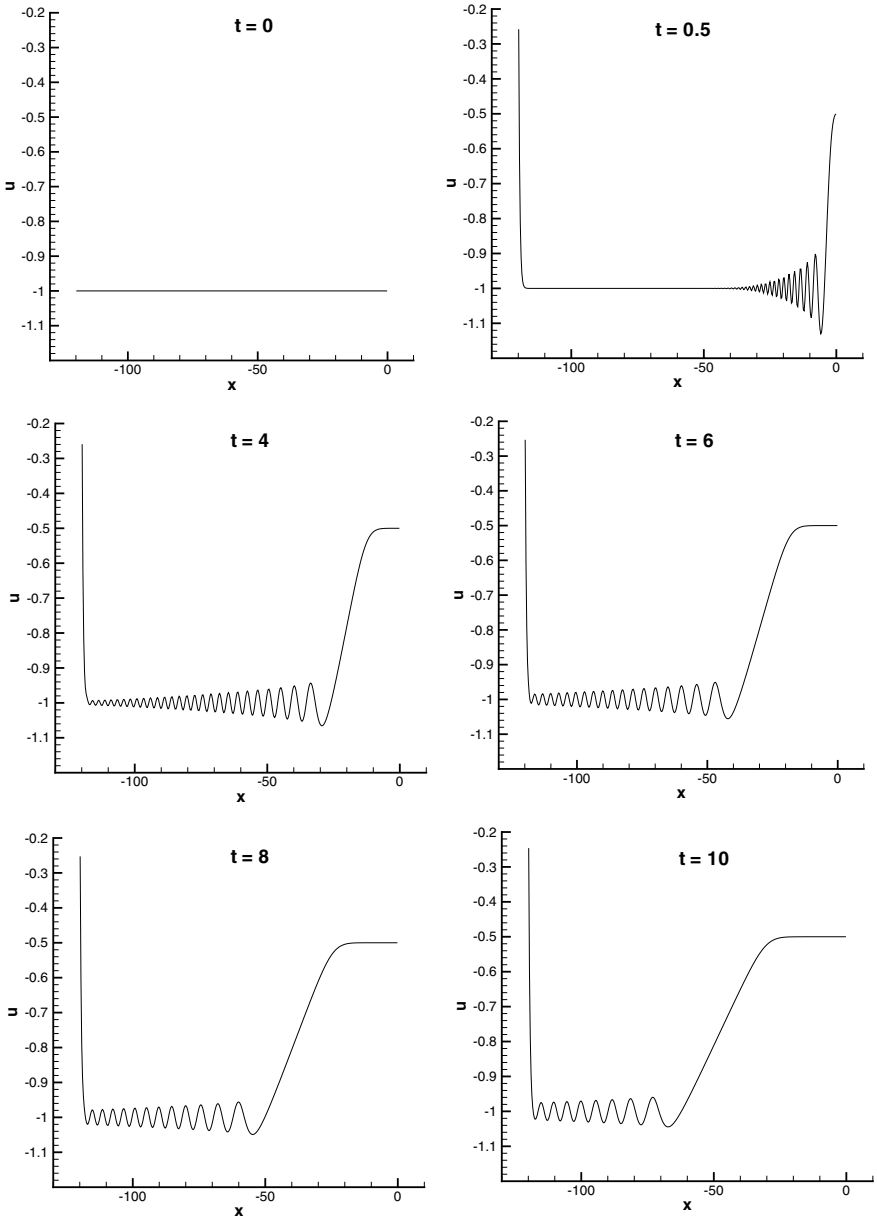

Fig. 5. $u_0(x) = -1.0$, $u(-120, t) = 0$, $u(0, t) = -0.5$, $u_x(0, t) = 0$ with P^1 polynomial and 400 cells, at $t = 0$, 0.5, 4, 6, 8, and 10.

Example IV. For this case, the initial and boundary data are of the form

$$\begin{cases} u_0(x) = -1.0, & x \in [-120, 0], \\ a(t) = -0.5, & t > 0, \\ b(t) = 0, & t > 0. \end{cases} \tag{4.3}$$

Here the right boundary data is negative $a(t) = -0.5$ and its value is bigger than the initial data $u_0 \leqslant a < 0$, as discussed in Section 4 the wave pattern should have the form (4.5). Our numerical solution is shown in Fig. 5, and the result is consistent with the analysis. Near the right boundary solution is just a uniform shelf equals to right boundary value $a(t) = -0.5$, a linear function is formed in the middle to connect to the left smaller initial data, which is similar to Example III, and for $x < 6u_0t$, the solution behaves more like a constant close to the initial data.

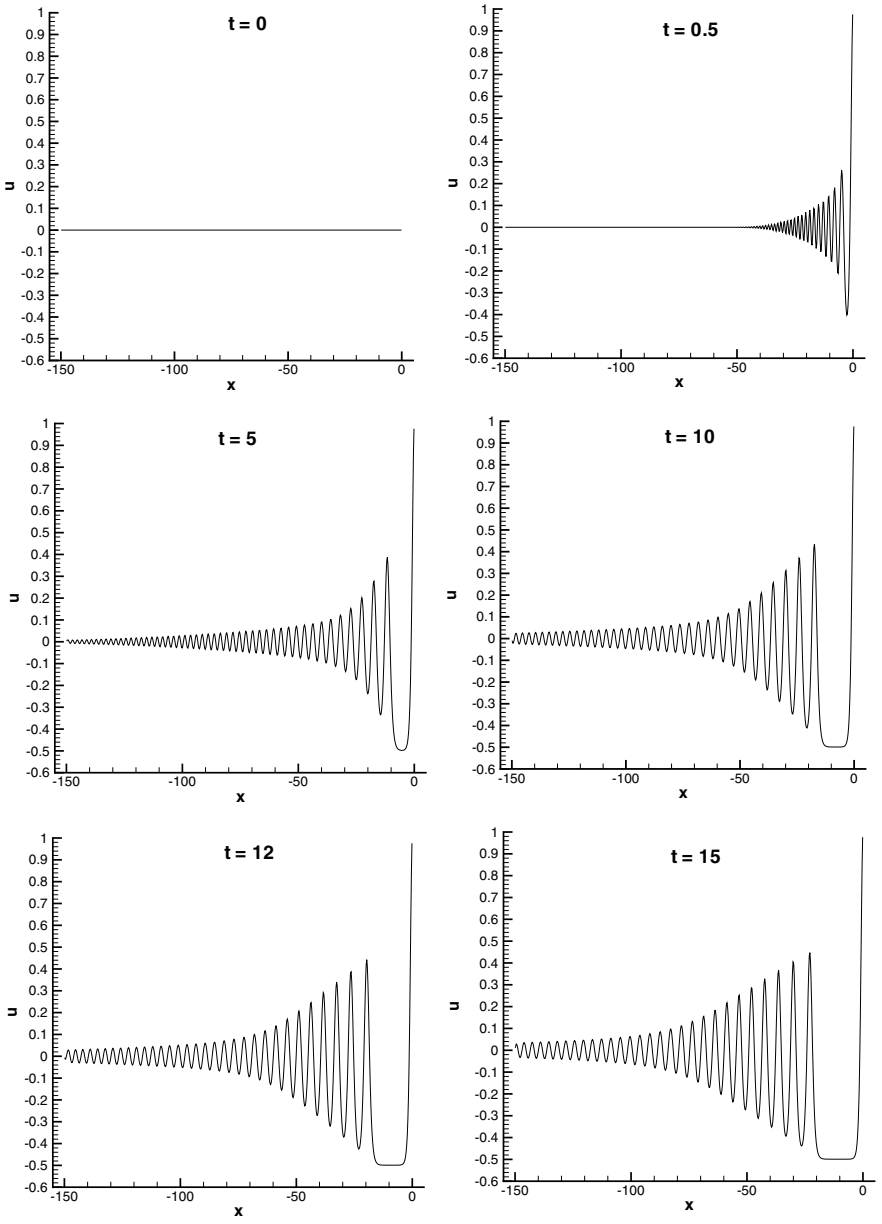

Fig. 6. $u_0(x) = 0$, $u(-150, t) = 0$, $u(0, t) = 1$, $u_x(0, t) = 0$ with P^1 polynomial and 600 cells, at $t = 0$, 0.5, 5, 10, 12, and 15.

Example V. For this case, the initial and boundary data are of the form

$$\begin{cases} u_0(x) = 0, & x \in [-150, 0], \\ a(t) = 1.0, & t > 0, \\ b(t) = 0, & t > 0. \end{cases} \tag{4.4}$$

Here the right boundary data is positive $a(t) = 1.0$ and its value to initial data satisfies $-\frac{a}{2} < u_0 < \frac{a}{4}$, from Section 4 we know that the wave pattern should have the form (4.3). Our numerical solution is shown in Fig. 6, and the result is consistent with the analysis. Half of a soliton wave is formed near the right boundary, an undular bore is formed in the middle to connect to the left smaller initial data, and for $x < 6(u_0 + a)t$ the solution behaves more like a constant close to the initial data.

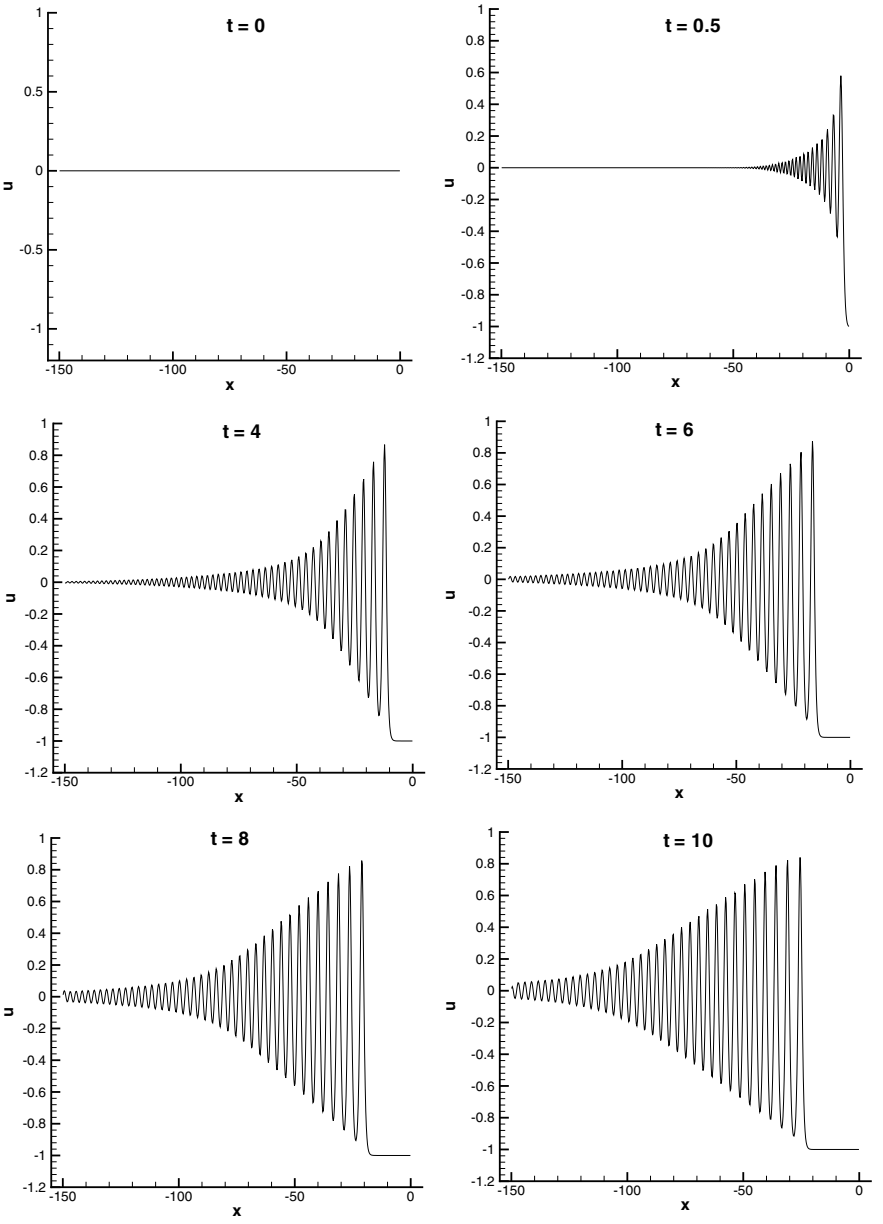

Fig. 7. $u_0(x) = 0$, $u(-150, t) = 0$, $u(0, t) = -1$, $u_x(0, t) = 0$ with P^1 polynomial and 600 cells, at $t = 0$, 0.5, 4, 6, 8, and 10.

Example VI. In this example the initial and boundary data are of the form

$$\begin{cases} u_0(x) = 0, & x \in [-150, 0], \\ a(t) = -1, & t > 0, \\ b(t) = 0, & t > 0. \end{cases} \tag{4.5}$$

Here the right boundary data is negative $a(t) = -1.0$ and its value to initial data satisfies $a < u_0 < -\frac{a}{2}$. As discussed in Section 4 we know the wave pattern should have the form (4.6). Our numerical solutions are shown in Fig. 7, and the results are consistent with the analysis. Near the right boundary a uniform shelf equals to right boundary data is formed, an undular bore is formed in the middle to connect to the left larger initial data and for $x < 6(2a - u_0)t$, the solution behaves more like a constant close to the initial data.

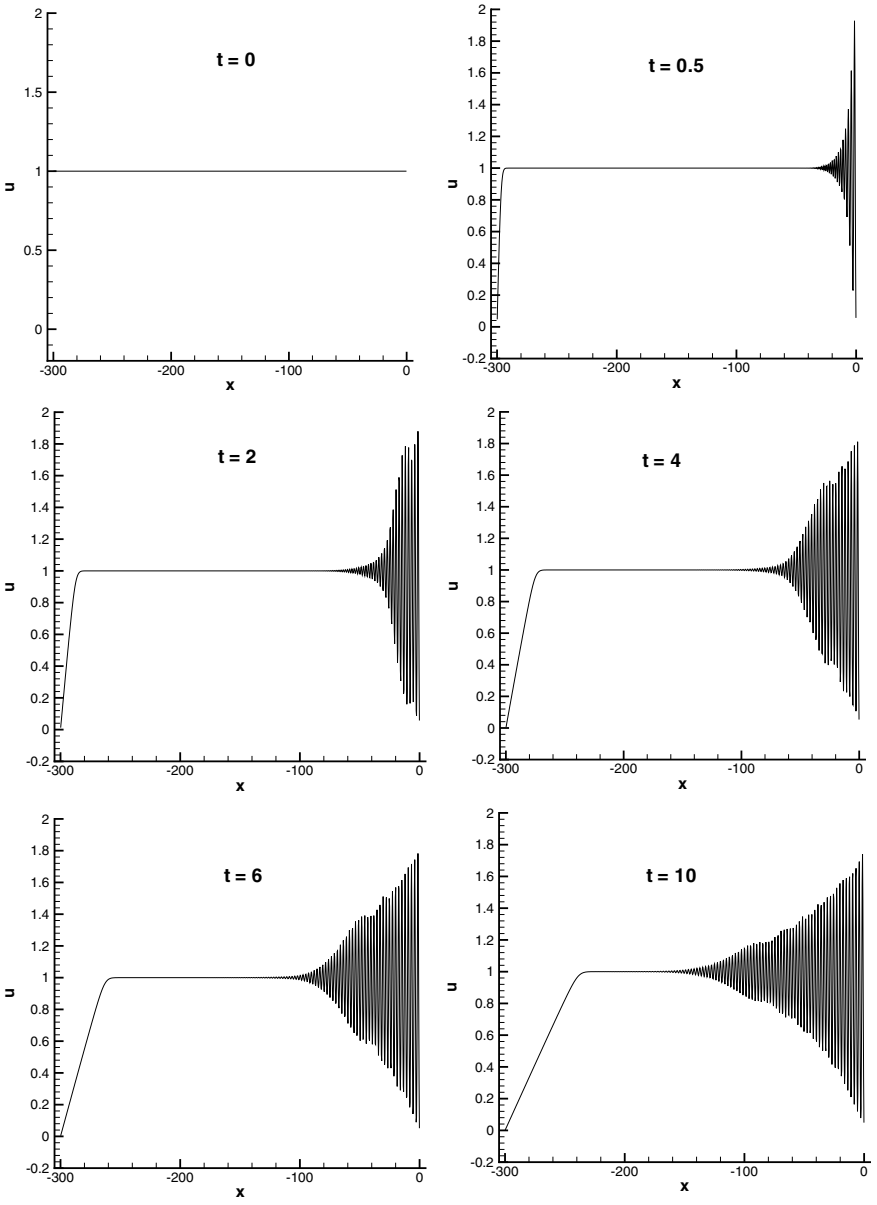

Fig. 8. $u_0(x) = 1$, $u(-300, t) = 0$, $u(0, t) = 0$, $u_x(0, t) = 0$ with P^1 polynomial and 1000 cells, at $t = 0$, 0.5, 2, 4, 6, and 10.

Table 4
The L^2 norm at different time for Example VII with P^1 polynomials

L^2 norm	$T=0$	$T=0.5$	$T=1$	$T=2$	$T=4$	$T=6$	$T=8$	$T=10$
$n=1000$	1.0000	0.9977	0.9964	0.9919	0.9792	0.9645	0.9493	0.9340

Example VII. For this case, the initial and boundary data are of the form

$$\begin{cases} u_0(x) = 1, & x \in [-300, 0], \\ a(t) = 0, & t > 0, \\ b(t) = 0, & t > 0. \end{cases} \tag{4.6}$$

As we see the right boundary data and initial data satisfy the inequality $u_0 > \frac{1}{4}a$ and $u_0 > -\frac{1}{2}a$, so as discussed in Section 4 we know that the wave pattern should have the form (4.4), a conoidal wave should be formed near the right boundary matched to a partial undular bore. Our numerical solutions are shown in Fig. 8. We do observe a conoidal wave formed near the right boundary matched to a partial undular bore to further connect to the left bigger initial data. Since the solution has strong oscillatory wave patterns, we also compute the L^2 energy norm in Table 4, we see the energy is well conserved, which is consistent with the L^2 stability analysis 3.1.

6. Conclusion remarks

We have introduced a systematic LDG method for computing dispersive wave equations posed on a negative quarter-plane or finite domain, using the KdV equation as a canonical testing example. In our approach, non-homogeneous boundary conditions are first converted into homogeneous boundary conditions by a simple transformation, a LDG method is then derived through an auxiliary problem. The inter-cell fluxes and the boundary fluxes are chosen to ensure stability and to incorporate the given boundary conditions.

Our method can be applied to a class of problems arising in surface water waves, plasma waves where the computation of boundary wave patterns is desirable. Recently there has been an increasing interest in the study of initial boundary problems for dispersive wave equations, see e.g. [3,19,28,4,26,29,15,25]. The techniques discussed in this paper are very well suited for handling equations with high-order derivatives and non-homogeneous boundary conditions.

Acknowledgements

We are grateful to Professors Chi-Wang Shu and Marshall Slemrod for stimulating discussions. Liu's research is partially supported by the NSF under grant DMS05-05975 and the Ames Laboratory, Department of Energy (DOE). The work of Yan was supported in part by ONR Grant N00014-03-1-0071.

References

[1] J.L. Bona, W.G. Pritchard, L.R. Scott, An evaluation of a model equation for water waves, Philos. Trans. Roy. Soc. London Ser. A 302 (1471) (1981) 457–510.
[2] J.L. Bona, S.-M. Sun, B.-Y. Zhang, The initial boundary-value problem for the KdV equation on a quarter plane, Trans. Amer. Math. Soc. 354 (2001) 427–490.
[3] J.L. Bona, S.M. Sun, B.-Y. Zhang, Forced oscillations of a damped Korteweg–de Vries equation in a quarter plane, Commun. Contemp. Math. 5 (3) (2003) 369–400.
[4] J.L. Bona, S.M. Sun, B.-Y. Zhang, A nonhomogeneous boundary-value problem for the Korteweg–de Vries equation posed on a finite domain, Comm. Partial Differential Equations 28 (7–8) (2003) 1391–1436.
[5] J.L. Bona, R. Winther, The Korteweg–de Vries equation, posed in a quarter-plane, SIAM J. Math. Anal. 14 (6) (1983) 1056–1106.
[6] B.A. Bubnov, Generalized boundary value problems for the KdV equation in bounded domain, Differential Equations 15 (1979) 17–21.
[7] B.A. Bubnov, Solvability in the large of nonlinear boundary value problems for the KdV equations, Differential Equations 16 (1980) 24–30.
[8] R. Camassa, T. Yao-tsu Wu, The Korteweg–de Vries equation with boundary forcing, Wave Motion 11 (1989) 495–506.

[9] X.-L. Chu, L.W. Xiang, Y. Baransky, Solitary waves induced by boundary motion, Comm. Pure Appl. Math. 36 (1983) 495–504.
[10] S.R. Clarke, J. Imberge, Nonlinear effects in the unsteady, critical withdrawal of a stratified fluid, in: Fourth International Symposium on Stratified Flows, LEGI, 1994, pp. 1–8.
[11] B. Cockburn, C.-W. Shu, The local discontinuous Galerkin method for time-dependent convection–diffusion systems, SIAM J. Numer. Anal. 35 (6) (1998) 2440–2463 (electronic).
[12] B. Cockburn, C.-W. Shu, Runge–Kutta discontinuous Galerkin methods for convection-dominated problems, J. Sci. Comput. 16 (3) (2001) 173–261.
[13] J.E. Colliander, C.E. Kenig, The generalized KdV equation on the half plane, Commun. Partial Differential Equations 27 (2002) 2187–2266.
[14] M.D. Kruskal, C.S. Gardner, J.M. Green, R.M. Miura, Method for solving Korteweg–de Vries equation, Phys. Rev. Lett. 19 (1967) 1095–1098.
[15] A.S. Fokas, Ehrenpreis type representations and their Riemann–Hilbert nonlinearisation, J. Nonlinear Math. Phys. 10 (Suppl. 1) (2003) 47–61.
[16] A.S. Fokas, M.J. Ablowitz, Forced nonlinear evolution equations and the inverse scattering transform, Stud. Appl. Math. 80 (3) (1989) 253–272.
[17] B. Fornberg, G.B. Whitham, A numerical and theoretical study of certain nonlinear wave phenomena, Philos. Trans. Roy. Soc. London Ser. A 289 (1361) (1978) 373–404.
[18] G.L. Lamb Jr., Elements of Soliton Theory, John Wiley, New York, 1980.
[19] B.-Y. Guo, J. Shen, On spectral approximations using modified Legendre rational functions: application to the Korteweg–de Vries equation on the half line, Indiana Univ. Math. J. 50 (Special Issue) (2001) 181–204, Dedicated to Professors Ciprian Foias and Roger Temam (Bloomington, IN, 2000).
[20] A.V. Gurevich, L.P. Pitayevskiĭ, Nonstationary structure of a collisionless shock wave, Sov. Phys. JETP 33 (1974) 291–297.
[21] W.-Z Huang, D.M. Sloan, The pseudospectral method for third-order differential equations, SIAM J. Numer. Anal. 29 (6) (1992) 1626–1647.
[22] S. Kichenassamy, P.J. Olver, Existence and nonexistence of solitary wave solutions to high-order model evolution equations, SIAM J. Appl. Math. 23 (1992) 1141–1166.
[23] H.-O. Kreiss, J. Lorenz, Initial-boundary value problems and the Navier–Stokes equationsClassics in Applied Mathematics, vol. 47, SIAM, Philadelphia, PA, 2004 (reprint of the 1989 edition).
[24] D. Levy, C.-W. Shu, J. Yan, Local discontinuous Galerkin methods for nonlinear dispersive equations, J. Comput. Phys. 196 (2) (2004) 751–772.
[25] H. Liu, M. Slemrod, KdV dynamics in the plasma-sheath transition, Appl. Math. Lett. 17 (4) (2004) 401–410.
[26] H.-P. Ma, W.-W. Sun, A Legendre–Petrov–Galerkin and Chebyshev collocation method for third-order differential equations, SIAM J. Numer. Anal. 38 (5) (2000) 1425–1438 (electronic).
[27] H.-P. Ma, W.-W. Sun, Optimal error estimates of the Legendre–Petrov–Galerkin method for the Korteweg–de Vries equation, SIAM J. Numer. Anal. 39 (4) (2001) 1380–1394 (electronic).
[28] T.R. Marchant, N.F. Smyth, The initial boundary problem for the Korteweg–de Vries equation on the negative quarter-plane, Proc. Roy. Soc. London Ser. A Math. Phys. Eng. Sci. 458 (2020) (2002) 857–871.
[29] J. Shen, A new dual-Petrov–Galerkin method for third and higher odd-order differential equations: application to the KdV equation, SIAM J. Numer. Anal. 41 (5) (2003) 1595–1619 (electronic).
[30] C.-W. Shu, S. Osher, Efficient implementation of essentially nonoscillatory shock-capturing schemes, J. Comput. Phys. 77 (2) (1988) 439–471.
[31] G.B. Whitham, Linear and Nonlinear Waves, in: Pure and Applied Mathematics, Wiley–Interscience, John Wiley, New York, 1974.
[32] Y. Xu, C.-W. Shu, Local discontinuous Galerkin methods for nonlinear Schrödinger equations, J. Comput. Phys. 205 (2005) 52–97.
[33] J. Yan, C.-W. Shu, A local discontinuous Galerkin method for KdV type equations, SIAM J. Numer. Anal. 40 (2) (2002) 769–791 (electronic).
[34] J. Yan, C.-W. Shu, Local discontinuous Galerkin methods for partial differential equations with higher order derivatives, in: Proceedings of the Fifth International Conference on Spectral and High Order Methods, ICOSAHOM-01, Uppsala, J. Sci. Comput. 17 (2002) 27–47.